

Ces anions cycliques P_3O_9 et les molécules d'eau sont liées par des ponts hydrogène dont le détail est donné dans le Tableau 2. Il est à noter que l'atome d'oxygène O(E22) agit deux fois en tant qu'accepteur. A l'intérieur du réseau formé par les anions P_3O_9 et les molécules d'eau, les cations associés Ba et Na ont des polyèdres de coordination formés de six atomes d'oxygène et trois molécules d'eau dans le cas du baryum, six atomes d'oxygène et une molécule d'eau dans le cas du sodium.

Il est à noter que l'un des atomes d'oxygène de liaison du cycle P_3O_9 [O(L23)] participe à la coordination de l'atome de sodium, constatation peu usuelle dans le cas des phosphates condensés.

Acta Cryst. (1987). C43, 392–395

Potassium Gallotitanogallate, $K_x[Ga_{2+x}Ti_{2-x}O_7](x \leq 0.25)$

BY MAMORU WATANABE, TAKAYOSHI SASAKI, YOSHIZO KITAMI AND YOSHINORI FUJIKI

National Institute for Research in Inorganic Materials, Namiki 1-1, Sakura-mura, Niihari-gun, Ibaraki 305, Japan

(Received 21 July 1986; accepted 1 October 1986)

Abstract. $M_r = 355.6$ ($x \sim 0.14$), tetragonal, $I4/m$, $a = 18.135$ (2), $c = 2.9966$ (4) Å, $V = 985.5$ (2) Å³, $Z = 8$, $D_m = 4.69$, $D_x = 4.79$ Mg m⁻³, $\lambda(\text{Mo } K\alpha) = 0.71069$ Å, $\mu = 15.2$ mm⁻¹, $F(000) = 1327$, $T = 298$ K, $R = 4.36\%$ for 726 unique reflections. The structure consists of rutile- and β -gallia-type structural columns parallel to the c axis which are alternately arrayed on the (001) plane and mutually joined with octahedral and tetrahedral apexes. Large one-dimensional tunnels surrounded by four octahedron strips and four tetrahedron chains occur along the column axis. These tunnels are 6.2 Å in diameter and have a smooth inside wall, in which K ions are accommodated.

Introduction. This compound has an ionic conductivity of about 1 kS m⁻¹ even at room temperature in the microwave range where mobile ions show clearly their response to the intrinsic barriers for ion diffusion (Yoshikado, 1987; Yoshikado, Ohachi, Taniguchi, Onoda, Watanabe & Fujiki, 1983). The value is about 100 times larger than those reported for ionic conductors like $\text{Na}\beta\text{-Al}_2\text{O}_3$. This new structure, therefore, is very interesting crystallographically from the viewpoint of ion conduction phenomena.

Experimental. Fibrous crystals ($x \sim 0.14$) were grown from a flux melt of $\text{K}_2\text{CO}_3\text{-MoO}_3$ containing TiO_2 and Ga_2O_3 . The density was obtained by measuring the buoyancy of crystallites of about 300 mg in CCl_4 at

Références

- Enraf-Nonius (1977). *Structure Determination Package*. Enraf-Nonius, Delft.
International Tables for X-ray Crystallography (1974). Tome IV. Birmingham: Kynoch Press. (Distributeur actuel D. Reidel, Dordrecht.)
 MARTIN, C. & DURIF, A. (1972). *Bull. Soc. Fr. Minéral. Cristallogr.* **95**, 149–153.
 MARTIN, C. & MITSCHLER, A. (1972). *Acta Cryst.* **B28**, 2348–2352.
 SEETHANEN, D., DURIF, A. & GUITEL, J. C. (1977). *Acta Cryst.* **B33**, 2716–2719.
 STOUT, G. H. & JENSEN, L. H. (1968). *Structure Determination*. London: Macmillan.

room temperature. A nearly cylindrical crystal, 0.03 × 0.2 mm in size, was used for taking Laue and Weissenberg photographs and measuring diffraction intensities on a Rigaku four-circle automatic diffractometer (AFC-5). The photographs gave an extinction rule of $h + k + l = 2n$ with Laue symmetry $4/m$. Twenty reflections with $40 < 2\theta < 55^\circ$ were used for measuring lattice parameters. Intensity measurements were carried out in the range $-28 \leq h \leq 28$, $0 \leq k \leq 28$, $0 \leq l \leq 4$ below 0.9 \AA^{-1} in $\sin\theta/\lambda$ by the ω - 2θ scanning method at a speed of 1° min^{-1} with Lp effects automatically corrected. Maximum fluctuation of three standard reflections was 1.2% throughout experiment. 1840 reflections were measured and averaged to 936 non-equivalents containing 210 reflections less than $3\sigma(F_o)$; $R_{\text{int}} = 4.83\%$. Maximum and minimum transmission factors of cylindrical absorption correction were 0.668 and 0.626. The structure was solved by Patterson maps and a (001) high-resolution lattice image, shown in Fig. 1, which was taken at $\sim 800 \text{ \AA}$ underfocus near the optimum value ($\sim 900 \text{ \AA}$) using 80 beams within an objective aperture of 0.4 \AA^{-1} in JEM 4000-FX (JEOL). The image was used to pick up metal-metal vectors from the maps and to ascertain their relative positions in the (001) projection. It was shown clearly on the Patterson sections with $z = 0$ and $\frac{1}{2}$ whether these vectors were parallel to (001) or not. The O positions were found on the basis of the concept of anion packing from the Patterson and difference Fourier maps. The function $\sum w(|F_o| - |F_c|)^2$ was

minimized in a least-squares refinement, with $w = 1/\sigma(F_o)^2$. Atomic positions, anisotropic thermal parameters and a scale factor were refined, resulting in $R = 4.36\%$ and $wR = 2.87\%$ with an isotropic extinction parameter of 3.6×10^{-4} : the 002 reflection was omitted because the intensity was $\sim 25\%$ less than that calculated in spite of a very strong reflection. Maximum and minimum $\Delta\rho$ are 0.5 and $-0.6 \text{ e } \text{\AA}^{-3}$. Scattering factors and anomalous-dispersion factors were taken from *International Tables for X-ray Crystallography* (1974). Programs used were *ACACA* (Wuensch & Prewitt, 1965), *RSSF5* (Sakurai, 1967), *RADY* (Sasaki, 1982) and *BADTEA* (Finger & Prince, 1975).

Discussion. Atomic coordinates and equivalent isotropic thermal parameters are listed in Table 1* and selected metal–oxygen and oxygen–oxygen bond lengths in Table 2.

* Lists of structure factors and anisotropic thermal parameters have been deposited with the British Library Document Supply Centre as Supplementary Publication No. SUP 43456 (5 pp.). Copies may be obtained through The Executive Secretary, International Union of Crystallography, 5 Abbey Square, Chester CH1 2HU, England.

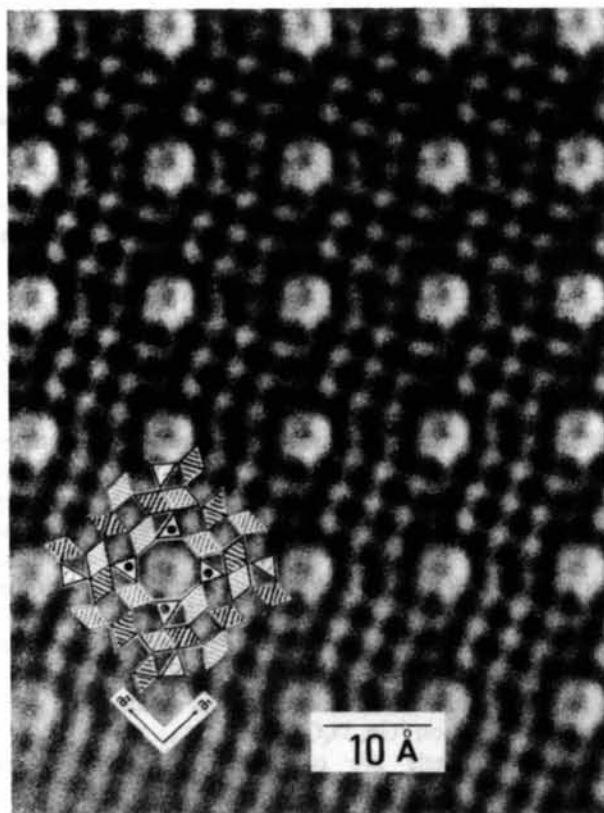


Fig. 1. (001) high-resolution lattice image of $K_x[Ga_{2+x}Ti_{2-x}O_7]$. Large white blobs correspond to octagonal tunnels.

As shown in Fig. 2, the structure consists of columnar elements of rutile and β -gallia (Geller, 1960) parallel to the c and b axes, respectively. Both types of column are alternately arrayed on the (001) plane in equal numbers reflecting the chemical composition and mutually linked by O(3), O(4), O(6) and O(7) at the corners of octahedra and tetrahedra. Octagonal tunnels which are surrounded by four octahedron strips from the rutile columns and four tetrahedron chains from the gallia columns occur along the unique axis. The strips are made by edge-sharing and the chains by corner-sharing.

Table 1. Atomic coordinates and equivalent isotropic thermal parameters

$$B_{eq} = \frac{1}{3} \sum_i \beta_i a_i^2$$

	Position	x	y	z	$B_{eq} (\text{\AA}^2)$
K	4(e)	0	0	0.242 (9)	8.0 (14)
Ga(M1)	8(h)	0.16218 (5)	0.11819 (5)	0.5	0.36 (4)
Ga/Ti(M2)	8(h)	0.31089 (6)	0.20322 (6)	0	0.41 (4)
Ti/Ga(M3)	8(h)	0.03559 (7)	0.22118 (8)	0	0.57 (5)
Ti(M4)	8(h)	0.54276 (9)	0.11930 (9)	0	0.58 (6)
O(1)	8(h)	0.0201 (3)	0.4102 (3)	0	0.60 (24)
O(2)	8(h)	0.1507 (3)	0.3950 (3)	0.5	0.49 (24)
O(3)	8(h)	0.0019 (3)	0.2803 (3)	0.5	0.60 (24)
O(4)	8(h)	0.1314 (3)	0.2645 (3)	0	0.56 (24)
O(5)	8(h)	0.2369 (3)	0.1892 (3)	0.5	0.44 (23)
O(6)	8(h)	0.0673 (3)	0.1558 (3)	0.5	0.58 (25)
O(7)	8(h)	0.1689 (3)	0.0613 (3)	0	0.76 (25)

Table 2. Selected metal–oxygen and oxygen–oxygen bond lengths (Å)

K–O(5)	3.173 (8) × 4	M3–O(2)	1.941 (4) × 2
–O(7)	3.338 (8) × 4	–O(4)	1.906 (6)
		–O(6)	1.995 (4) × 2
M1–O(5)	1.869 (6)	–O(7 ⁱⁱ)	1.996 (6)
–O(6)	1.852 (6)		Av. 1.962
–O(7)	1.823 (3) × 2		
	Av. 1.842	O(2)–O(2)	2.9966 (4)
O(5)–O(6)	3.136 (8)	O(2)–O(4)	2.800 (7) × 2
O(5)–O(7)	3.025 (7) × 2	O(2)–O(6)	2.550 (8) × 2
O(6)–O(7)	2.929 (7) × 2	O(2)–O(7 ⁱⁱⁱ)	2.763 (7) × 2
O(7)–O(7)	2.9966 (4)	O(4)–O(6)	2.735 (7) × 2
	Av. 3.007	O(6)–O(6)	2.9966 (4)
		O(6)–O(7 ⁱⁱⁱ)	2.781 (7) × 2
			Av. 2.771
M2–O(3 ⁱⁱⁱ)	1.912 (6)		
–O(4 ⁱⁱⁱ)	1.920 (3) × 2	M4–O(1 ⁱⁱⁱ)	1.957 (4) × 2
–O(5)	2.027 (4) × 2	–O(1 ⁱⁱ)	1.993 (6)
–O(5 ⁱⁱⁱ)	2.135 (6)	–O(2 ⁱⁱⁱ)	1.991 (6)
	Av. 1.990	–O(3 ⁱⁱ)	1.961 (4) × 2
			Av. 1.970
O(3 ⁱⁱⁱ)–O(4 ⁱⁱⁱ)	2.822 (7) × 2	O(1 ⁱⁱ)–O(1 ⁱⁱⁱ)	2.796 (7) × 2
O(3 ⁱⁱⁱ)–O(5 ⁱⁱⁱ)	2.955 (7) × 2	O(1 ⁱⁱⁱ)–O(1 ⁱⁱⁱ)	2.9966 (4)
O(4 ⁱⁱⁱ)–O(4 ⁱⁱⁱ)	2.9966 (4)	O(1 ⁱⁱⁱ)–O(2 ⁱⁱⁱ)	2.811 (7) × 2
O(4 ⁱⁱⁱ)–O(5 ⁱⁱⁱ)	2.532 (8) × 2	O(1 ⁱⁱⁱ)–O(3 ⁱⁱⁱ)	2.815 (7) × 2
O(4 ⁱⁱⁱ)–O(5)	2.788 (7) × 2	O(1 ⁱⁱⁱ)–O(3 ⁱⁱ)	2.524 (8) × 2
O(5)–O(5)	2.9966 (4)	O(2 ⁱⁱⁱ)–O(3 ⁱⁱ)	2.752 (7) × 2
O(5)–O(5 ⁱⁱⁱ)	2.708 (9) × 2	O(3 ⁱⁱ)–O(3 ⁱⁱⁱ)	2.9966 (4)
	Av. 2.800		Av. 2.782

Symmetry codes: (i) $x, y, 0$; (ii) $-y, x, 0$; (iii) $-x + \frac{1}{2}, -y + \frac{1}{2}, \frac{1}{2}$; (iv) $-y + \frac{1}{2}, x + \frac{1}{2}, \frac{1}{2}$; (v) $y + \frac{1}{2}, -x + \frac{1}{2}, \frac{1}{2}$.

All atoms except for K are placed on mirror planes with $z=0$ and $\frac{1}{2}$. The K^+ ions are located statistically and equivalently at $0, 0, \pm z$ and $\frac{1}{2}, \frac{1}{2}, \frac{1}{2} \pm z$ in the octagonal tunnels and have thermal ellipsoids unusually elongated in the channel direction; $z=0.242$, $\beta_{11}=0.003$ and $\beta_{33}=0.436$. They cannot stay simultaneously at $0, 0, \pm z$ or $\frac{1}{2}, \frac{1}{2}, \frac{1}{2} \pm z$ owing to steric hindrance between them. This means that their maximum content is two per unit cell, or $x \leq 0.25$ from crystallographic considerations.

$M1$ tetrahedral and $M4$ octahedral sites are preferentially occupied by Ga and Ti atoms, respectively. $M2$ sites accommodate the remaining Ti and Ga atoms in the ratio of 17 to 83, and the ratio for $M3$ sites is 69 to 31. Additional Ga^{3+} ions, corresponding to the x in the chemical formula, are concentrated in the $M3$ octahedra close to K^+ ions introduced with them in place of Ti^{4+} . With all this concentration of Ga^{3+} , the average metal–oxygen and oxygen–oxygen bond distances of the $M3$ octahedra are significantly smaller than those of $M4$ octahedra. The off-center displacements (Δ_M) of $M4$, $M3$ and $M2$ cations become larger in that order despite little difference in octahedron regularity (Δ_O) as shown in Table 3. The factors Δ_M and Δ_O are the dispersions of bond distances of metal–oxygen and oxygen–oxygen contact bondings in a coordination polyhedron: $\Delta_M = (1/n) \sum [(R - \bar{R}_i)^2 / \bar{R}_i^2]$ (Watanabe, Fujiki, Kanazawa & Tsukimura, 1986) and $\Delta_O = (1/n) \sum [(R - \bar{R})^2 / \bar{R}^2]$ (Shannon, 1976). This tendency of Δ_M holds also for $Ga_4Ti_{21}O_{48}$ (Lloyd, Grey & Bursill, 1976) which has a similar construction of β -gallia and

Table 3. Comparisons of octahedron regularities and off-center displacements among $K_x[Ga_{2+x}Ti_{2-x}O_7]$ and related compounds

	$K_xGa_{2+x}Ti_{2-x}O_7$	β - Ga_2O_3	TiO_2	$Ga_4Ti_{21}O_{48}$
Octahedron regularities (Δ_O)				
GaO_6	5.40×10^{-4}	5.2×10^{-4}	—	0.7×10^{-4}
GaO_6	3.05×10^{-3}	2.2×10^{-3}	—	1.2×10^{-3}
(Ti,Ga) O_6	2.21×10^{-3}	—	—	1.9×10^{-3}
TiO_6	2.49×10^{-3}	—	2.15×10^{-3}	$1.8-2.3 \times 10^{-3}$
Off-center displacements (Δ_M)				
GaO_6	1.14×10^{-4}	1.0×10^{-4}	—	2.0×10^{-4}
GaO_6	1.24×10^{-3}	7.8×10^{-4}	—	1.2×10^{-3}
(Ti,Ga) O_6	2.97×10^{-4}	—	—	1.5×10^{-4}
TiO_6	2.08×10^{-6}	—	0	$0-1.5 \times 10^{-5}$

rutile columns and hexagonal tunnels instead of octagonal ones. The Δ_M shows that the off-centering of $M2$ cations is remarkable among the three, and comparable off-center displacements are made in the corresponding octahedra in β -gallia and $Ga_4Ti_{21}O_{48}$ also. This large value of Δ_{M2} is attributed to a large off-edge displacement of an $M2$ cation from the shared edge with the equivalent $M2$ octahedron (e.g. the $M2^{iii}$ octahedron adjacent to the $M2^i$, where superscripts refer to symmetry codes), which is considered to take place mainly for relaxation of the Coulombic repulsive interaction between these $M2$ cations. By comparison with $M2$ and $M3$ cations, $M4$ cations are involved in very small off-centering and are placed in much more pseudosymmetrical surroundings by the first-neighboring cations (e.g. $M2^v$, $M3^{iii}$, $M4^{iv}$ and $M4^v$ about $M4^i$) although all $M2$ to $M4$ sites are of the same symmetry level, or $8(h)$ sites. It may be said that the variation of Δ_M among octahedra is correlated to how symmetrically a given octahedron is linked by the first-neighboring polyhedra.

O atoms form anion packing close to h.c.p., if extra O atoms are assumed to be in the tunnels. The packing planes are (210) and $(\bar{1}20)$ which correspond to (100) and (010) in rutile. The octahedra linkage in this structure can be derived from the rutile structure by the concept of crystallographic shear operations introduced by Wadsley (1964). The required operations are $(210)_r[\frac{1}{2}\frac{1}{2}1]_r$ and $(\bar{1}20)_r[\frac{1}{2}\frac{1}{2}1]_r$ in rutile index, and they take place every 2.5 rutile units for both $(210)_r$ and $(\bar{1}20)_r$. The octagonal tunnels are formed at all crosspoints of both operations. Each component operation has the ability to form hexagonal tunnels arrayed periodically on the defect line (Lloyd, Grey & Bursill, 1976; Bursill, 1979). When it operates at the above intervals, the rutile structure is divided into slabs with composition $[Ga_4Ti_9O_{24}]_n$.

Large tunnels are outlined by eight-membered oxygen rings on the (001)-projected figure which consist of two similar squares levelled at $z=0$ and $\frac{1}{2}$ and mutually twisted by about 45° around the channel axis. The squares are 6.2 and 6.5 Å in diagonal length

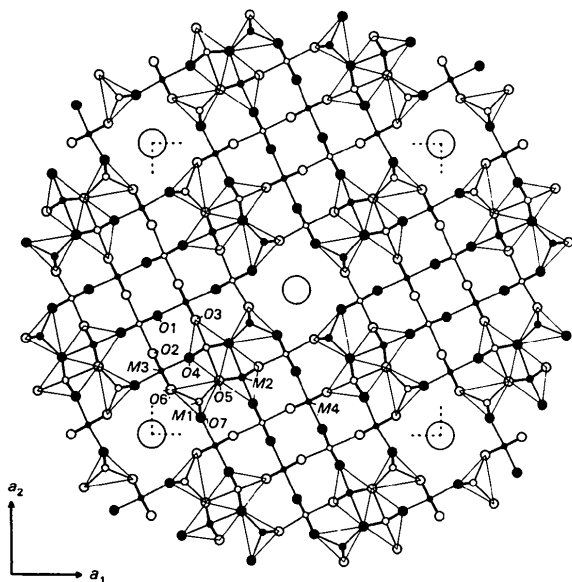


Fig. 2. (001) projection of the structure. Large, medium and small circles represent potassium, oxygen and titanium or gallium atoms, respectively. Dark and open circles represent $z=0$ and $\frac{1}{2}$, respectively (except for K atoms). β -Gallia regions are outlined by thin lines.

and are stacked alternately at a half period of the c axis. These diameters are considerably larger than those of one-dimensional tunnels in the other compounds, e.g. beryl (~ 5.2 Å), K_xWO_3 (~ 5.5 Å) and priderites (~ 5.3 Å) (Watanabe, Fujiki, Kanazawa & Tsukimura, 1986). If one assumes 1.40 Å for the oxygen radius, the net diameter of the present tunnels is 3.4 Å, comparable to the effective size of the eight-coordinated Cs ion (Shannon, 1976). It is suggested that such ions as K and Rb have no virtual bottlenecks for their translation in the tunnels, which is very interesting from the viewpoint of one-dimensional ion conduction phenomena. This subject will be described elsewhere in comparison with the hollandite-type tunnels in priderites (Watanabe, Sasaki, Kitami & Fujiki, 1986).

One of the authors (MW) is grateful to Drs Y. Kanazawa and K. Tsukimura, Geological Survey of Japan, for fruitful discussions and allowing us to use computation programs and to Dr Y. Bando, National Institute for Research in Inorganic Materials, for useful advice on taking lattice images.

Acta Cryst. (1987). **C43**, 395–397

Single-Crystal Neutron Diffraction Study of Hydrogen Bonding in Selenic Acid

BY H. ERFANY-FAR, H. FUESS AND D. GREGSON

Institut für Kristallographie der Universität, Senckenberganlage 30, D-6000 Frankfurt 1, Federal Republic of Germany

(Received 9 May 1986; accepted 7 October 1986)

Abstract. H_2SeO_4 , $M_r = 144.98$, orthorhombic, $P2_12_12_1$, $Z = 4$, $F(000) = 94.8 \times 10^{-15}$ m, $\lambda(\text{neutron}) = 1.1757(1)$ Å, $\mu = 0.11$ mm $^{-1}$. $T = 243$ K: $a = 8.476(5)$, $b = 8.123(5)$, $c = 4.585(4)$ Å, $V = 315.7$ Å 3 , $D_x = 3.05$ Mg m $^{-3}$. $T = 80$ K: $a = 8.449(5)$, $b = 8.118(5)$, $c = 4.588(4)$ Å, $V = 314.7$ Å 3 , $D_x = 3.06$ Mg m $^{-3}$. 519 ($T = 243$ K) and 308 ($T = 80$ K) diffractometer data; final $R = 0.052$, $wR = 0.051$ (243 K) and $R = 0.032$, $wR = 0.041$ (80 K). Hydrogen atoms were located and well ordered at both temperatures. Tetrahedral SeO_4 groups are connected by hydrogen bonds with O...O distances of 2.615(5) and 2.621(4) Å at 243 K to four neighbouring groups and form layers parallel to (100).

Introduction. The crystal structure of selenic acid was determined by Bailey & Wells (1951) from X-ray data. A neutron diffraction study on polycrystalline H_2SeO_4 (Moodenbaugh, Hartt, Hurst, Youngblood, Cox & Frazer, 1983) reported hydrogen positions determined

References

- BURSILL, L. A. (1979). *Acta Cryst.* **B35**, 530–538.
 FINGER, L. W. & PRINCE, E. (1975). *Natl Bur. Stand. (US) Tech. Note No.* 854.
 GELLER, S. (1960). *J. Chem. Phys.* **33**, 676–684.
International Tables for X-ray Crystallography (1974). Vol. IV. Birmingham: Kynoch Press. (Present distributor D. Reidel, Dordrecht.)
 LLOYD, D. J., GREY, I. E. & BURSILL, L. A. (1976). *Acta Cryst.* **B32**, 1756–1761.
 SAKURAI, T. (1967). *Universal Computation Program System (UNICS)*. Tokyo: The Crystallographic Society of Japan.
 SASAKI, S. (1982). *RADY*. Programs derived from *ORFLS* and *RADIEL*. State Univ. New York, Stony Brook.
 SHANNON, R. D. (1976). *Acta Cryst.* **A32**, 751–767.
 WADSLEY, A. D. (1964). *Non-Stoichiometric Compounds*, edited by L. MANDELCOIN, pp. 98–209. New York: Academic Press.
 WATANABE, M., FUJIKI, Y., KANAZAWA, Y. & TSUKIMURA, K. (1986). *J. Solid State Chem.* In the press.
 WATANABE, M., SASAKI, T., KITAMI, Y. & FUJIKI, Y. (1986). *J. Solid State Chem.* In the press.
 WUENSCH, B. J. & PREWITT, C. T. (1965). *Z. Kristallogr.* **1**, 24–59.
 YOSHIKADO, S. (1987). In preparation.
 YOSHIKADO, S., OHACHI, T., TANIGUCHI, I., ONODA, Y., WATANABE, M. & FUJIKI, Y. (1983). *Solid State Ionics*, **9/10**, 1305–1310.

by profile analysis at 330 and 10 K. Our investigation was already in progress when the results of Moodenbaugh *et al.* became available. The aim of our study was essentially the same as that of the previous one: determination of hydrogen positions and search for a possible order–disorder transition.

Experimental. Single crystals of selenic acid were obtained following a procedure described by Gilbertson & King (1936). Selenic acid with some water (Merck) was used as starting material and dried for several days by pumping dry air over the liquid. Final crystallization was achieved by seeding the liquid at room temperature in a dry glove-box. The crystal used for data collection was deliquescent and of irregular shape with dimensions $3 \times 2 \times 2$ mm. It was sealed in a glass capillary and mounted in a closed-loop Displex cryostat. Data collection was performed on the four-circle $P32$ diffractometer at the reactor Siloë of the CENG, wavelength $\lambda = 1.1757(1)$ Å from Cu(200),